

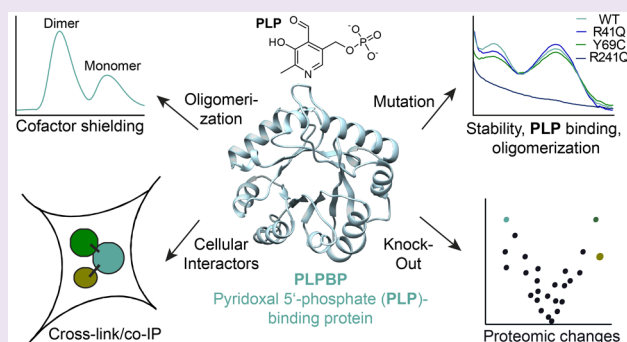
## Biochemical and Proteomic Studies of Human Pyridoxal 5'-Phosphate-Binding Protein (PLPBP)

Anja Fux<sup>†</sup> and Stephan A. Sieber<sup>\*,†</sup><sup>†</sup>Department of Chemistry, Chair of Organic Chemistry II, Center for Integrated Protein Science (CIPSM), Technische Universität München, Lichtenbergstraße 4, 85748 Garching, Germany

## Supporting Information

**ABSTRACT:** The pyridoxal 5'-phosphate-binding protein (PLPBP) is an evolutionarily conserved protein linked to pyridoxal 5'-phosphate-binding. Although mutations in PLPBP were shown to cause vitamin B6-dependent epilepsy, its cellular role and function remain elusive. We here report a detailed biochemical investigation of human PLPBP and its epilepsy-causing mutants by evaluating stability, cofactor binding, and oligomerization. In this context, chemical cross-linking combined with mass spectrometry unraveled an unexpected dimeric assembly of PLPBP. Furthermore, the interaction network of PLPBP was elucidated by chemical cross-linking paired with co-immunoprecipitation. A mass spectrometric analysis in a PLPBP knockout cell line resulted in distinct

proteomic changes compared to wild type cells, including upregulation of several cytoskeleton- and cell division-associated proteins. Finally, transfection experiments with vitamin B6-dependent epilepsy-causing PLPBP variants indicate a potential role of PLPBP in cell division as well as proper muscle function. Taken together, our studies on the structure and cellular role of human PLPBP enable a better understanding of the physiological and pathological mechanism of this important protein.



Pyridoxal 5'-phosphate (PLP) is a versatile cofactor enabling the catalysis of a plethora of chemical reactions, including decarboxylation, transamination, and racemization.<sup>1</sup> Because many essential cellular processes, such as glucose, lipid, and amino acid metabolism, are driven by PLP-dependent enzymes (PLP-DEs),<sup>2,3</sup> the functional assignment of uncharacterized members remains an important but so far very challenging task. For example, the human PLP-binding protein (PLPBP; previously proline synthase cotranscribed homologue, PROSC) was first described in 1999 and was demonstrated to be ubiquitously expressed in many tissues.<sup>4</sup> Although PLPBP is highly conserved with orthologs occurring across all domains of life, including plants and bacteria,<sup>4</sup> its exact cellular function is not defined. Although the protein binds PLP, no enzymatic activity toward any of the 20 proteinogenic amino acids, the main substrates of PLP-DEs, and their corresponding D-enantiomers was detected.<sup>5</sup> Instead, a role in PLP homeostasis was postulated as knockouts (KOs) of PLPBP orthologs, leading to increased pyridoxine toxicity in *Escherichia coli*<sup>6</sup> and cyanobacteria.<sup>7</sup> The reported pyridoxine toxicity, as well as increased valine secretions caused by the KO of the *E. coli* ortholog (*yggS*), can be complemented by human (PLPBP), yeast (*YBL036C*), and *Bacillus subtilis* (*ylmE*) variants, suggesting a largely conserved role.<sup>5,8</sup> While the protein is dispensable in several organisms, including *E. coli*,<sup>5,6</sup> cyanobacterium *Synechococcus elongates* (*pipY*),<sup>7</sup> zebrafish (*plpbb*), and human cancer cell lines,<sup>9</sup> it is essential in *Pseudomonas aeruginosa* (*PA0394*)<sup>10</sup> and possibly in other

pathogenic bacteria like *Helicobacter pylori* (*HP\_0395*) and *Staphylococcus aureus* (*ylmE*).<sup>6,11</sup> Human recombinant PLPBP has been reported to largely consist of monomers and a small amount of dimer.<sup>12</sup> Crystal structures are available for yeast<sup>13</sup> and some bacterial orthologs,<sup>5,14</sup> which support a monomeric state with a solvent-exposed cofactor. Because mechanisms of cofactor transport within the cell are still unknown, it was hypothesized that PLPBP could be involved in delivering PLP to apo-forms of vitamin B6-binding proteins.<sup>8,14,15</sup>

Mutations in human PLPBP have been linked to vitamin B6-dependent epilepsy (VitB6-EP).<sup>8,9,16,17</sup> In addition, PLPBP functions as a tumor suppressor gene in hepatocellular carcinoma (HCC)-derived cell lines.<sup>18</sup> KO studies suggest that PLPBP affects mitochondrial metabolism in yeast and leads to a significant reduction of systemic PLP and PL concentrations as well as altered amino acid levels in zebrafish.<sup>9</sup> Bacterial orthologs have been demonstrated to cluster with genes involved in cell division,<sup>6,7</sup> and an analysis of KO cells indicates a putative role in amino acid homeostasis,<sup>5–7</sup> which is in line with observations in zebrafish.<sup>9</sup> Although PLPBP-deficient HEK293 cells have been shown to display decreased PLP and increased PNP levels, there is no information on proteomic changes caused by a PLPBP KO. Moreover, the

Received: October 23, 2019

Accepted: December 11, 2019

Published: December 11, 2019

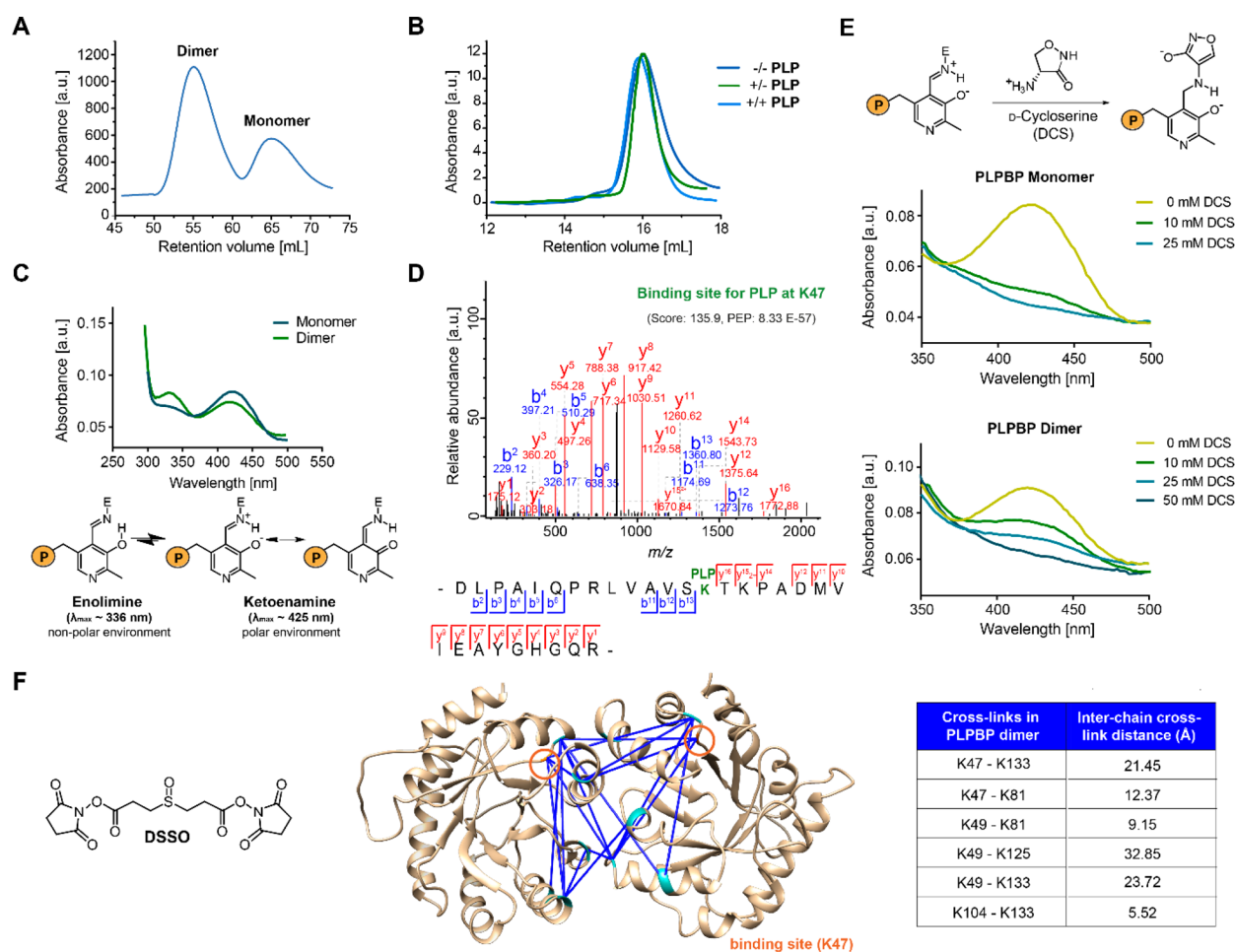


**Figure 1.** Properties of recombinant human PLPBP. (A) The main oligomeric state of tag-free PLPBP is dimeric, with a small fraction of monomer according to size-exclusion chromatography (SEC; preparative scale). (B) Preincubation of monomeric PLPBP with either excess PLP and separation in buffer without PLP (+/−) or in buffer containing PLP (+/+) or preincubation and separation in the absence of PLP (−/−; analytical scale); retention volume of dimer: approximately 13.82 mL). (C) UV/vis spectra of PLPBP monomer and dimer display characteristic absorbance peaks corresponding to the internal aldimine. Peak intensities resulting from the enolimine ( $\lambda_{\max} \approx 336$  nm) and ketoenamine ( $\lambda_{\max} \approx 425$  nm) forms of the internal aldimine were different for both monomers and dimers at equal concentrations ( $P = OPO_3^{2-}$ ).<sup>21</sup> (D) Tandem MS (MS/MS) spectra identifying the PLP-binding site of PLPBP (K47) with corresponding score and posterior error probability (PEP; false discovery rate, FDR < 0.01). (E) Incubation with 10 mM of the PLP-binding antibiotic D-cycloserine (DCS) leads to almost complete displacement of PLP from monomeric PLPBP, whereas 50 mM DCS was required for the PLPBP dimer ( $P = OPO_3^{2-}$ ).<sup>22</sup> (F) Analysis of PLPBP by chemical cross-linking combined with mass spectrometry (XL-MS) utilizing the DSSO cross-linker (left). Cross-links solely occurring in the dimer peak after treatment (right, two independent samples (50- and 100-fold excess DSSO) with two fragmentation strategies each, FDR < 0.01) served as restraints for molecular docking of two PLPBP monomers (derived from SWISS-MODEL<sup>23</sup> using the yeast ortholog as template, PDB 1B54<sup>13</sup>) using HADDOCK<sup>24</sup> to generate a dimer model (center). Median  $\text{Ca}-\text{Ca}$  cross-link distances are all within the maximum distance span of DSSO (35 Å). Lysine residues involved in cross-linking contacts are highlighted cyan, and the PLP binding site is colored orange.

cellular interaction partners of human PLPBP are unknown. Therefore, although possible cellular roles of PLPBP have been discussed, a clear picture of its functions still remains elusive.

Here, we elucidate the oligomeric state of human PLPBP *via* chemical cross-linking combined with mass spectrometry (XL-MS). In contrast to previous observations, our data reveal that the protein is predominantly dimeric, shielding the cofactor from the environment. Furthermore, we investigated the oligomerization behavior as well as the stability of mutants causing VitB6-EP where we observed significant differences among the variants. To gain deeper insights into its functional role, we performed *in situ* chemical cross-linking followed by co-immunoprecipitation (cross-link/co-IP)<sup>19</sup> and unraveled proteins associated with cytoskeleton organization as interaction partners. Moreover, a PLPBP KO human cell line results in signature proteome changes with downregulation of

two PLP-DEs important for H<sub>2</sub>S production and upregulation of cytoskeleton-associated proteins. Finally, the transfection of the KO cell line with VitB6-EP-associated mutants revealed insights into pathological phenotypes, including alterations in the expression of proteins essential for cell division and muscle function.

## RESULTS AND DISCUSSION

**Unusual Oligomerization Properties of Human PLPBP.** In order to access human PLPBP for functional studies, we expressed and purified Strep-tag or tag-free recombinant human PLPBP. Size-exclusion chromatography (SEC) revealed that the protein independent of the presence of the affinity tag is predominantly dimeric even under reductive conditions excluding the role of disulfide bonds in this process (Figures 1A and S1A).<sup>20</sup> This observation differs

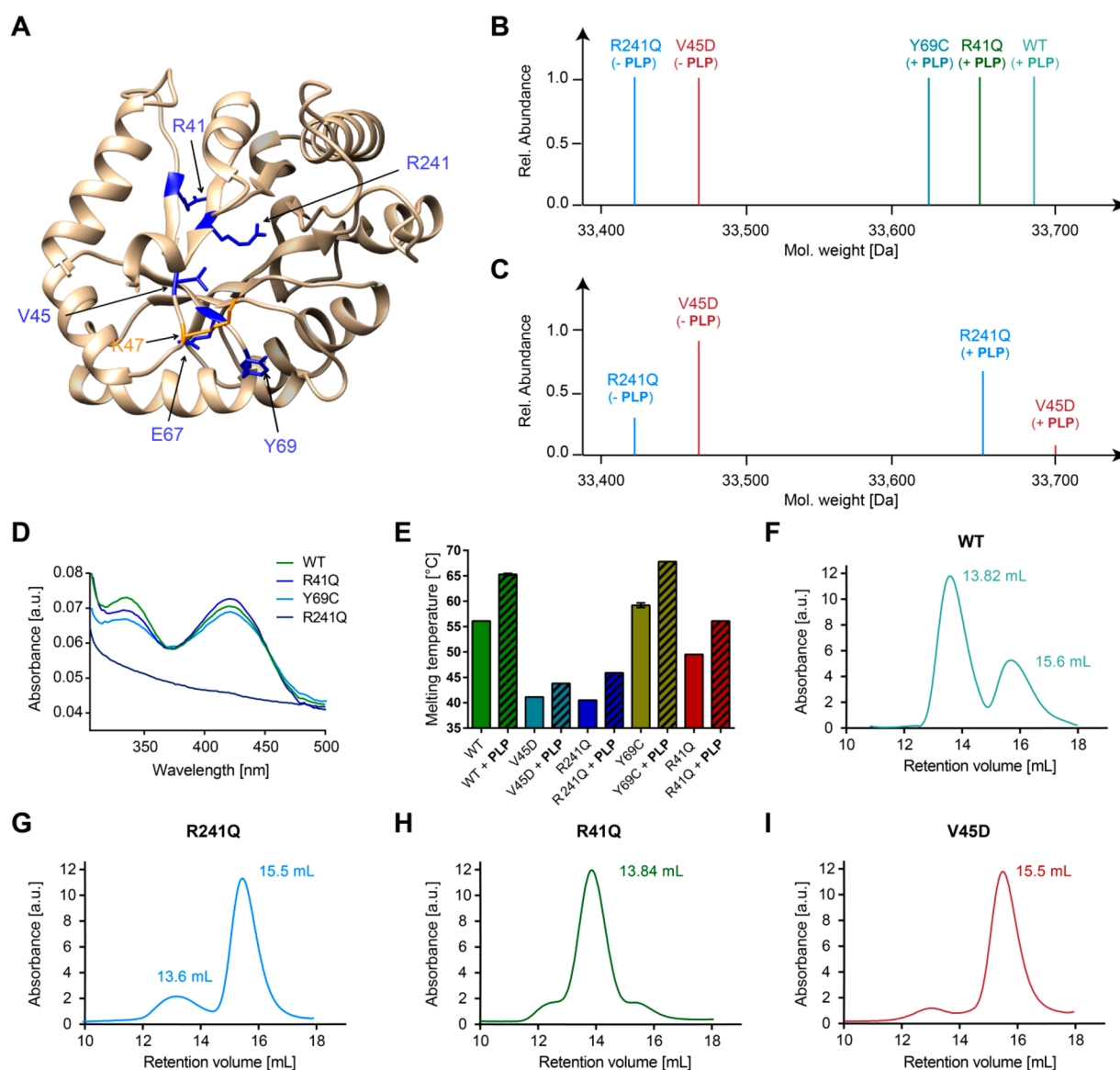


**Figure 2.** Impact of pathogenic mutations on PLPBP cofactor binding, stability, and oligomerization. (A) Localization of mutated residues (blue) on the human wild type PLPBP model structure (derived from SWISS-MODEL<sup>23</sup> using the yeast ortholog as template, PDB 1B54<sup>13</sup>). The PLP-binding site (K47) is colored orange. (B) Intact-protein MS of WT and mutants after reduction with NaBH<sub>4</sub>. (C) Intact-protein MS of V45D and R241Q mutants after incubation with a 4-fold molar excess of PLP followed by NaBH<sub>4</sub> reduction. (D) UV/vis spectra of PLPBP WT and mutants. (E) Thermal stability of PLPBP WT and mutants in the absence or presence of PLP (20-fold molar excess). (F–I) Analytical size-exclusion chromatograms of WT, R241Q, R41Q, and V45D mutants under reductive conditions, respectively.

from previous results postulating that human PLPBP largely exists as a monomer with only a minor fraction of dimer present.<sup>12</sup> A possible explanation could be differences in expression strains and purification strategies that might have affected the monomer-to-dimer ratio. For instance, we here applied Strep-tag affinity purification, whereas previous studies applied immobilized metal affinity chromatography (IMAC). In addition, we performed SEC directly after affinity chromatography to separate the monomer and dimer as well as remove the aggregated protein. However, the isolation of the separated monomer and dimer peaks and reanalysis by size-exclusion chromatography did not affect oligomerization, indicating that both species are stable and not in rapid equilibrium (Figure S1B and C). Furthermore, dimerization was not dependent on the addition of PLP (Figures 1B and S1D). We confirmed that both the monomeric and dimeric

species bind PLP by high-resolution MS (MW = 33684 Da with Strep-tag, MW = 30479 Da without tag) and UV/vis spectroscopy, where both displayed the characteristic internal aldimine peaks ( $\lambda_{\max} \approx 336$  nm and  $\lambda_{\max} \approx 425$  nm,<sup>21</sup> Figure 1C). Lys47 was determined the PLP-binding site of PLPBP *via* liquid chromatography combined with tandem MS (LC-MS/MS) analysis after reduction of the PLP adduct to the secondary amine using NaBH<sub>4</sub> (Figure 1D).

Because yeast (PDB 1B54)<sup>13</sup> and several other bacterial PLPBP orthologs are monomeric proteins,<sup>14</sup> a predominantly dimeric species suggests a characteristic property and possibly indicates an additional evolved function or special regulatory mechanism of human PLPBP. In monomeric PLPBP orthologs like *E. coli* YggS (PDB 1W8G) the cofactor is solvent exposed.<sup>14</sup> In order to compare the solvent accessibility of human dimeric and monomeric PLPBP, we incubated both

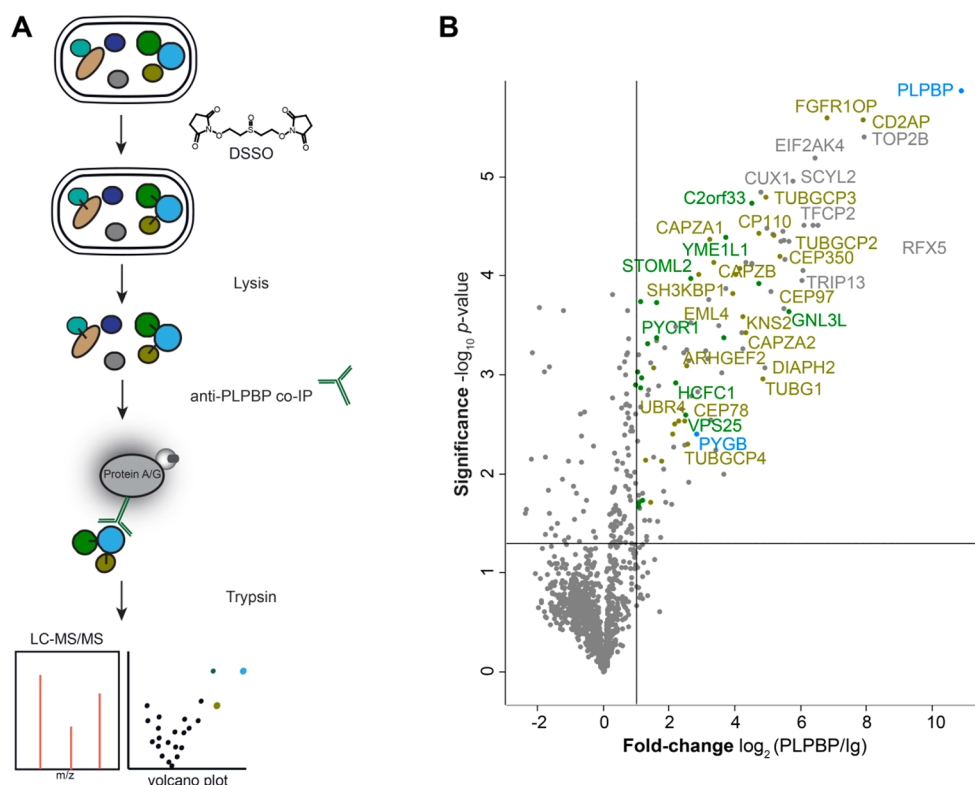


**Figure 3.** Cross-link/co-IP against human PLPBP from HEK293. (A) Combined cross-link/co-IP workflow applying the membrane-permeable DSSO cross-linker on intact cells prior to lysis and pull-down. Enriched proteins were digested and measured by LC-MS/MS. (B) Volcano plot representing *t*-test results of anti-PLPBP co-IP compared to the isotype control (Ig) co-IP ( $n = 4$  biological replicates). Cutoff values were defined as enrichment factor of  $\log_2(\text{PLPBP/Ig}) = 1$  (2-fold enrichment) and  $-\log_{10}(p\text{-value}) = 1.3$  (solid lines). Significantly enriched mitochondrial proteins are highlighted in green, PLP-DEs in blue, and proteins connected to the cytoskeleton in other.

species with increasing concentrations of the PLP-binding antibiotic D-cycloserine (DCS)<sup>25</sup> and monitored the absorbance at 425 nm (Figures 1E and S1E–F).<sup>22</sup> The internal aldimine of the monomer was almost completely lost upon incubation with 10 mM DCS. In contrast, the dimer aldimine was observed up to a concentration of 50 mM DCS. Further, the peak intensities resulting from the enolimine ( $\lambda_{\text{max}} \approx 336$  nm) and ketoenamine ( $\lambda_{\text{max}} \approx 425$  nm) forms of the internal aldimine were different in monomer and dimer species (Figure 1C).<sup>21</sup> In line with DCS titration, these differences suggest a reduced solvent exposure of PLP in dimeric PLPBP compared to the monomer, as the enolimine form is favored in a nonpolar environment.

To inspect the dimerization interface of PLPBP more closely, we performed XL-MS using the MS-cleavable cross-linker DSSO (Figure 1F, left).<sup>26</sup> The PLPBP dimer was efficiently stabilized upon DSSO addition (50-fold excess over PLPBP, reaction time of 1 h at 37 °C) as determined by SDS-PAGE (Figure S1G). Notably, monomeric PLPBP did not form dimers after incubation with DSSO (Figure S1H). The treated dimer and monomer fractions were separated by SEC prior to reduction, alkylation, and digestion (Figure S1I). Cross-linked peptides were measured by LC-MS/MS, and the data were analyzed using XlinkX (Table S1).<sup>19,27</sup> A PLPBP monomer crystal structure was modeled using the SWISS-MODEL platform with the ortholog from yeast (PDB 1B54<sup>13</sup>) as a template.<sup>23,28</sup> Cross-links solely occurring in the dimer fraction served as restraints for the generation of a PLPBP dimerization model with the software tool HADDOCK (Figure 1F, center).<sup>24</sup> Dimer cross-links mapped onto the

model are all within the maximum distance span of DSSO (35 Å; Figure 1F, right).<sup>29</sup> The involvement of the PLP-binding site K47 in cross-linking suggests that a certain fraction of PLP binding lysine residues is, at least temporarily, free of the cofactor and thereby able to react with DSSO. In line with UV/vis data, the PLPBP dimer model displayed an oligomerization interface located around the PLP-binding site K47, resulting in cofactor shielding upon PLPBP oligomerization. In this way, the predominant dimer conformation of human PLPBP would be in line with a function of shielded transport or storage of PLP in the cell.

**Biochemical Properties of VitB6-EP-Associated Mutants.** To address how mutations causing VitB6-EP impact cofactor binding and oligomerization of PLPBP, we selected previously expressed Y69C and R241Q<sup>12</sup> as well as uncharacterized R41Q, E67K, and V45D variants that are all located around the PLP-binding site K47 (Figure 2A). Notably, all mutants except E67K could be successfully obtained *via E. coli* expression but with a markedly reduced yield compared to wild type (WT) PLPBP (Figure S2A). The MS analysis of NaBH<sub>4</sub>-reduced proteins revealed that Y69C and R41Q mutants are fully saturated with PLP after purification, which is in line with the UV/vis analysis (the yield of V45D was too low for absorbance determination; Figure 2B and D). In contrast, R241Q and V45D did not bear any cofactor, confirming the role of these residues in PLP binding (Figure 2B and D).<sup>9</sup> However, the incubation with a 4-fold molar excess of PLP prior to reduction and MS analysis resulted in the appearance of holo-V45D and -R241Q in addition to the cofactor free species, suggesting that both are



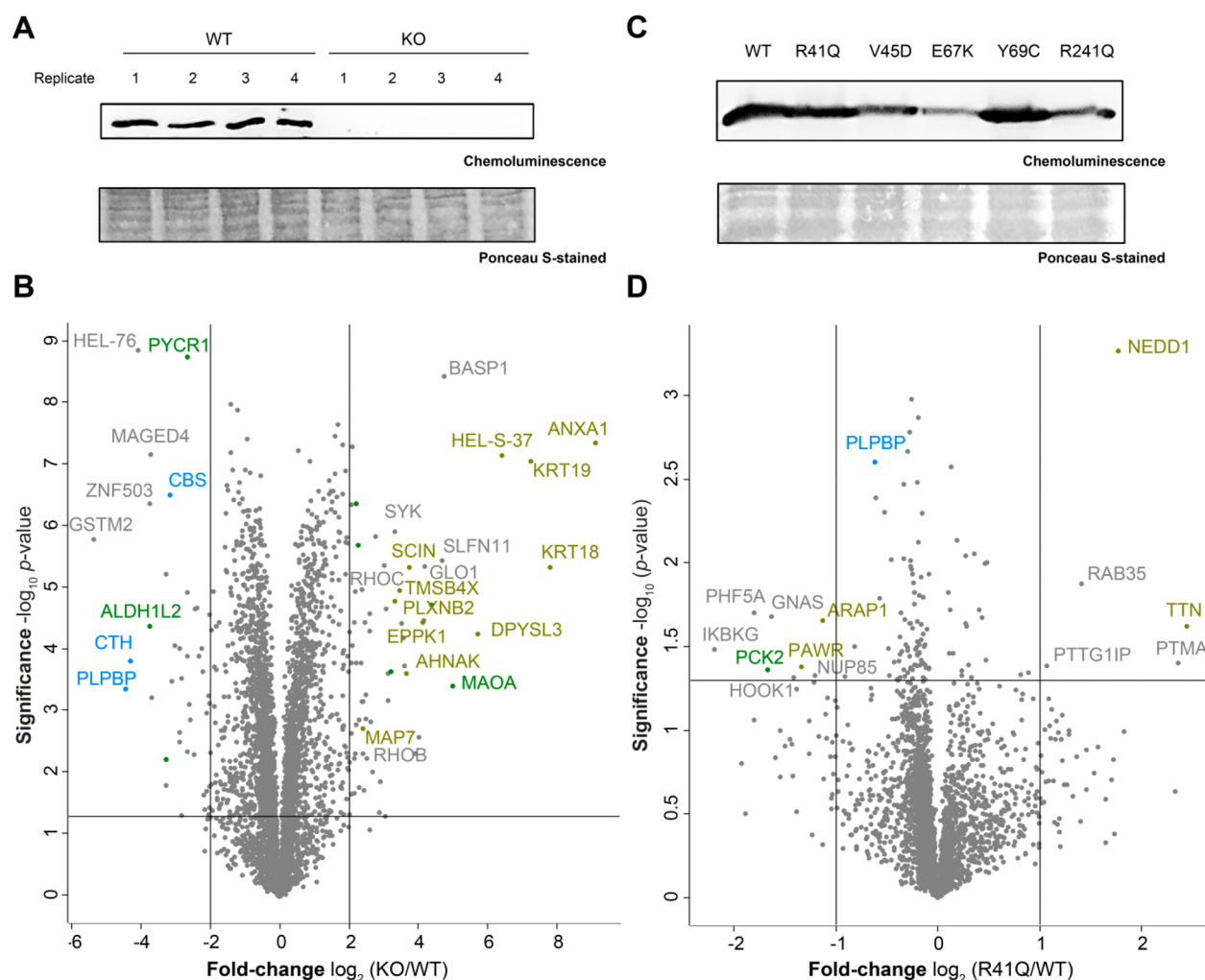


**Figure 4.** Proteomic changes upon PLPBP KO and mutant expression in HEK293. (A) Western blot analysis of PLPBP KO and WT cells using an anti-PLPBP antibody. (B) Volcano plot representing *t*-test results of HEK293 PLPBP KO cells compared to HEK293 wild type control cells ( $n = 4$  biological replicates). Cutoff values were defined as enrichment factor of  $\log_2(\text{KO}/\text{WT}) = 2$  (4-fold enrichment) or depletion factor of  $\log_2(\text{KO}/\text{WT}) = -2$  (4-fold depletion) and  $-\log_{10}(p\text{-value}) = 1.3$  (solid lines). Dysregulated mitochondrial proteins are highlighted in green, PLP-DEs in blue, and proteins connected to the cytoskeleton in other. (C) Western blot analysis of transfection of PLPBP WT and mutants into HEK293 PLPBP KO cells using an anti-FLAG antibody. (D) Volcano plot representing *t*-test results of overexpression of the R41Q mutant compared to overexpression of the WT in PLPBP KO cells ( $n = 4$  biological replicates). Cutoff values were defined as enrichment factor of  $\log_2(\text{R41Q}/\text{WT}) = 1$  (2-fold enrichment) or depletion factor of  $\log_2(\text{R41Q}/\text{WT}) = -1$  (2-fold depletion) and  $-\log_{10}(p\text{-value}) = 1.3$  (solid lines). Dysregulated mitochondrial proteins are highlighted in green, PLP-DEs in blue, and proteins connected to the cytoskeleton in other.

able to bind the cofactor when PLP is applied at high concentrations (Figure 2C). We further compared the thermal stabilities of PLPBP mutants and WT in the presence and absence of PLP (Figure 2E). In line with MS data and UV/vis spectra, mutants lacking PLP displayed overall lower melting temperatures in the range of 40 °C. R41Q, which is bound to PLP, exhibited reduced stability (49.5 °C) compared to the WT (56.1 °C), whereas the Y69C substitution resulted in a slight melting temperature increase (59.2 °C).<sup>12</sup> PLP had a stabilizing effect on all variants. In the next step, we evaluated the oligomerization behavior of the PLPBP mutants under reductive conditions (Figures 2F–I and S2B). Interestingly, all variants except the R41Q substitution are exclusively present in their monomeric state, with a slight residual amount of the dimer state in regards to the R241Q mutant. Even under nonreductive conditions the Y69C mutant did not form dimers contrary to previous postulations (Figure S2C).<sup>12</sup> Different oligomerization behaviors may be attributed to the location of

amino acids within the PLPBP dimerization region (Figure S2D). For example, while R41 is located most distant from lysine residues involved in cross-linking contacts within the PLPBP dimer, Y69C is directly placed at the interface, thereby providing an explanation for why its mutation leads to a strong monomerization. The pathological mutations (except for R41Q), therefore, all lead to the monomerization of PLPBP, which suggests that this dimer-to-monomer transition is important for pathology.

**Cellular Interaction Network of PLPBP.** To elucidate the cellular role of PLPBP *via* its interaction network, we treated a human embryonic kidney cell line (HEK293) with the cell-permeable DSSO cross-linker and performed co-IP against PLPBP (Figure 3A).<sup>19</sup> Most PLPBP interactors within HEK293 are cytosolic proteins (~85%; GO term 0005737: cytoplasm;<sup>30</sup> Figure 3B, Table S2). The occurrence of both cytosolic and mitochondrial interactors is in line with immunochemical staining revealing that PLPBP is present in

cytosol as well as mitochondria.<sup>9</sup> We did not observe an overrepresentation of PLP-DEs among the PLPBP-binding proteins (GO term 0030170: PLP-binding<sup>30</sup>), suggesting that PLPBP is not delivering PLP to apo-enzymes as previously proposed.<sup>8,14,15</sup> Interestingly, we detected a high number of proteins involved in cytoskeleton organization (almost 22%). These included components of the  $\gamma$ -tubulin ring complex necessary for microtubule nucleation at the centrosome (TUBGCP2–4),<sup>31</sup> proteins involved in centriole and spindle formation (CEP78, CEP97, CEP350, CP110),<sup>32–38</sup> or several subunits of the F-actin capping complex that regulate the growth of actin filaments (CAPZA1–A2, CAPZB).<sup>39</sup>

**Proteomic Effects of PLPBP KO and VitB6-EP-Associated Mutants.** We further examined the proteomic changes caused by a PLPBP KO in the HEK293 cell line compared to the WT cells. A Western blot analysis confirmed the previously reported KO (Figure 4A).<sup>9</sup> The morphology and growth rate of the WT and KO cells were similar to each other. Upon MS analysis (Figure 4B, Table S3), we observed an overexpression of several proteins involved in cytoskeleton organization like keratins (KRT18–19) or actin-binding proteins like annexins (ANXA1, ANXA3, and ANXA6) and plastin (HEL-S-37).<sup>40,41</sup> An alteration of expression levels of proteins associated with the cytoskeleton may provide a possible link to epileptic phenotypes observed in patients with VitB6-EP,<sup>8,9,16,17</sup> as proper integrity of cytoskeletal filaments is essential, e.g., for normal nervous system functionality and muscle growth.<sup>42,43</sup> Moreover, rho-related GTP-binding proteins (ROHB and ROHC) that determine the positioning of the contractile ring during mitosis<sup>44</sup> were upregulated. Interestingly, both cystathionine  $\gamma$ -lyase (CTH) and cystathionine  $\beta$ -synthase (CBS) were downregulated upon PLPBP KO. CTH and CBS are the two major sources for endogenous hydrogen sulfide (H<sub>2</sub>S), which is a signaling molecule that exerts multiple effects in most organs, including the nervous system and skeletal muscle.<sup>45,46</sup>

In the next step, we compared expression levels of the PLPBP WT and mutants after transfection into the PLPBP KO cells (Figure 4C). For the evaluation of proteomic changes caused by VitB6EP-linked variants, we selected the R41Q mutant, as this is the only PLPBP variant, which is still able to form dimers, and the V45D mutant, as its binding capacity for PLP is most significantly diminished (Figure 2). The expression levels of mutants after transfection, monitored by MS-based analysis (Figures 4D and S3, Table S3), are in line with the protein expression revealed by the Western blot analysis (Figure 4C). The proteome-related changes caused by the overexpression of the mutants compared to the WT transfected control (Figure 4D) were less pronounced than the alterations caused by the KO (Figure 4B), suggesting that the PLPBP biological function is largely retained. Interestingly, both mutants displayed differences in their up- and down-regulated proteins, which is in line with the different phenotypes caused by the variants.<sup>8,9,16,17</sup> However, the neural precursor cell expressed, developmentally downregulated protein 1 (NEDD1), a  $\gamma$ -tubulin ring complex-associated protein essential for proper cell division,<sup>47</sup> was upregulated upon expression of both variants. This is an interesting observation, as the proteins of the  $\gamma$ -tubulin ring complex (TUBGCP2–4) as well as  $\gamma$ -tubulin itself (TUBG1) were among the significantly enriched interactors of PLPBP (Figure

3B), reinforcing a possible role of PLPBP in cell division suggested by previous gene clustering analysis.<sup>6,7</sup>

## CONCLUSION

Here, we investigated the structural and cellular properties of human PLPBP. In contrast to previous observations, the protein is predominantly dimeric with a minor amount of monomer, which might be caused by different expression and purification strategies. Because cofactor accessibility is altered upon oligomerization, PLPBP might take the role of a PLP storage protein, which has been suggested previously.<sup>6,9,48</sup> This theory would be in line with earlier studies using a vitamin B6-mimicking probe to enrich human PLP-DEs. In all cell lines examined, PLPBP was a prominent hit, indicating a high affinity toward PLP.<sup>20</sup> Moreover, the expression levels of PLPBP in yeast and HeLa cells are almost 10-fold higher compared to the median protein copy number.<sup>49</sup> PLPBP deficiency could therefore markedly increase free cellular PLP levels. Because PLP exhibits a highly reactive aldehyde<sup>50</sup> and was reported as a member of the 30 most damage-prone metabolites,<sup>51</sup> detoxification by reduction to PNP might be a protective mechanism and explain the high PNP levels observed within PLPBP KO cells and in primary skin fibroblasts isolated from patients with VitB6-EP.<sup>9</sup> The altered stability, cofactor binding, and oligomerization underlined the pathological effects of epilepsy-associated PLPBP variants. The interacting networks of PLPBP from HEK293 examined by cross-link/co-IP revealed mainly cytosolic proteins, including a high number of cytoskeleton- and cell division-associated interactors. We did not observe an overrepresentation of PLP-DEs among the PLPBP interactors, which suggests that the protein is not involved in cofactor delivery to apo-vitamin B6-binding proteins, as proposed in previous studies.<sup>8,14,15</sup> KO of PLPBP in HEK293 resulted in significant upregulation of proteins associated with cytoskeleton organization and cell division, in line with the co-IP results. Moreover, the two PLP-DEs CTH and CBS, important for H<sub>2</sub>S synthesis, were downregulated. Because H<sub>2</sub>S exerts multiple effects on, for example, muscle and nervous system function, these proteomic results may provide a link to pathological mechanisms. Finally, global changes in cellular protein levels caused by the expression of PLPBP mutants strengthened a possible role in cell division and correct muscle integrity and function, as suggested by gene clustering analysis<sup>6,7</sup> and pathological phenotypes.<sup>8,9,16,17</sup> Because cellular protein function might also differ depending on the type of cell, an investigation of other cell lines may reveal additional information on PLPBP cellular roles. Taken together, we here report an in-depth study on human recombinant WT and mutant PLPBPs, revealing unprecedented insights into protein oligomerization as well as putative cellular roles.

## METHODS

All mass spectrometric data have been deposited at the ProteomeXchange Consortium (<https://www.ebi.ac.uk/pride/archive/>) via the PRIDE partner repository<sup>52</sup> with the data set identifier PXD015984. The authors declare that all other data supporting the findings of this study are available within the article and its SI files or from the corresponding author upon request.

## ■ ASSOCIATED CONTENT

### Supporting Information

The Supporting Information is available free of charge at <https://pubs.acs.org/doi/10.1021/acscchembio.9b00857>.

Table S2, which includes data for proteins significantly enriched upon PLPBP cross-link/co-IP from HEK293 (XLSX)

Table S3, which includes data for global proteome studies on PLPBP (XLSX)

Experimental procedures, including biochemical and biological methods, cell culture preparation, binding site identification of PLPBP, chemical XL-MS, and proteomic methods, and supporting figures and tables, including Table S1, cross-linking of PLPBP with a MS-cleavable DSSO linker; Figure S1, properties of recombinant human PLPBP; Figure S2, impact of pathogenic mutations on PLPBP cofactor binding, stability, and oligomerization; and Figure S3, proteomic changes upon V45D expression in HEK293 (PDF)

## ■ AUTHOR INFORMATION

### Corresponding Author

\*E-mail: [stephan.sieber@tum.de](mailto:stephan.sieber@tum.de).

### ORCID

Stephan A. Sieber: 0000-0002-9400-906X

### Author Contributions

A.F. designed, planned, and conducted all experiments, including protein expression and analytics, proteomics sample preparation, and chemical cross-linking experiments. A.F. performed the MS measurements and statistical analysis of the data. S.A.S. supervised the experiments. A.F. and S.A.S. wrote the manuscript.

### Funding

This project has received funding from the European Research Council (ERC) and the European Union's Horizon 2020 research and innovation program (Grant Agreement No. 725085, CHEMMINE, ERC consolidator grant). Further financial support was provided by the Deutsche Forschungsgemeinschaft (DFG) SFB 749.

### Notes

The authors declare no competing financial interest.

## ■ ACKNOWLEDGMENTS

We thank M. Wolff, K. Gliesche, and K. Bäuml for technical assistance. We thank V. Korotkov for synthesis of the DSSO cross-linker. We thank S. Houten (Icahn School of Medicine at Mount Sinai, New York, US) for supplying us with the HEK293 PLPBP KO cells. We thank S. Hacker and C. Gleissner for critical evaluation of the manuscript.

## ■ REFERENCES

- (1) Percudani, R., and Peracchi, A. (2003) A Genomic Overview of Pyridoxal-Phosphate-Dependent Enzymes. *EMBO Rep.* 4, 850–854.
- (2) Parra, M., Stahl, S., and Hellmann, H. (2018) Vitamin B6 and Its Role in Cell Metabolism and Physiology. *Cells* 7, 84.
- (3) Eliot, A. C., and Kirsch, J. F. (2004) Pyridoxal Phosphate Enzymes: Mechanistic, Structural, and Evolutionary Considerations. *Annu. Rev. Biochem.* 73, 383–415.
- (4) Ikegawa, S., Isomura, M., Koshizuka, Y., and Nakamura, Y. (1999) Cloning and Characterization of Human and Mouse PROSC (Proline Synthetase Co-Transcribed) Genes. *J. Hum. Genet.* 44, 337–342.

- (5) Ito, T., Iimori, J., Takayama, S., Moriyama, A., Yamauchi, A., Hemmi, H., and Yoshimura, T. (2013) Conserved Pyridoxal Protein That Regulates Ile and Val Metabolism. *J. Bacteriol.* 195, 5439–5449.
- (6) Prunetti, L., El Yacoubi, B., Schiavon, C. R., Kirkpatrick, E., Huang, L., Bailly, M., El Badawi-Sidhu, M., Harrison, K., Gregory, J. F., Fiehn, O., Hanson, A. D., and de Crecy-Lagard, V. (2016) Evidence That COG0325 Proteins Are Involved in PLP Homeostasis. *Microbiology (London, U. K.)* 162, 694–706.
- (7) Labella, J. I., Cantos, R., Espinosa, J., Forcada-Nadal, A., Rubio, V., and Contreras, A. (2017) PipY, a Member of the Conserved COG0325 Family of PLP-Binding Proteins, Expands the Cyanobacterial Nitrogen Regulatory Network. *Front. Microbiol.* 8, 1–16.
- (8) Darin, N., Reid, E., Prunetti, L., Samuelsson, L., Husain, R. A., Wilson, M., El Yacoubi, B., Footitt, E., Chong, W.K., Wilson, L. C., Prunty, H., Pope, S., Heales, S., Lascelles, K., Champion, M., Wassmer, E., Veggiotti, P., de Crecy-Lagard, V., Mills, P. B., and Clayton, P. T. (2016) Mutations in PROSC Disrupt Cellular Pyridoxal Phosphate Homeostasis and Cause Vitamin-B6-Dependent Epilepsy. *Am. J. Hum. Genet.* 33, 1–10.
- (9) Johnstone, D. L., Al-Shekaili, H. H., Tarailo-Graovac, M., Wolf, N. I., Ivy, A. S., Demarest, S., Roussel, Y., Ciapaite, J., van Roermund, C. W. T., Kernohan, K. D., Kosuta, C., Ban, K., Ito, Y., McBride, S., Al-Thihli, K., Abdelrahim, R. A., Koul, R., Al Futaisi, A., Haaxma, C. A., Olson, H., Sigurdardottir, L. Y., Arnold, G. L., Gerkes, E. H., Boon, M., Heiner-Fokkema, M. R., Noble, S., Bosma, M., Jans, J., Koolen, D. A., Kamsteeg, E.-J., Drogemoller, B., Ross, C. J., Majewski, J., Cho, M. T., Begtrup, A., Wasserman, W. W., Bui, T., Brimble, E., Violante, S., Houten, S. M., Wevers, R. A., van Faassen, M., Kema, I. P., Lepage, N., Lines, M. A., Dymont, D. A., Wanders, R. J. A., Verhoeven-Duif, N., Ekker, M., Boycott, K. M., Friedmann, J. M., Pena, I. A., and van Karnebeek, C. D. M. (2019) PLPBP Deficiency: Clinical, Genetic, Biochemical, and Mechanistic Insights. *Brain* 142, 542–559.
- (10) Rusmini, R., Vecchietti, D., Macchi, R., Vidal-Aroca, F., and Bertoni, G. (2014) A Shotgun Antisense Approach to the Identification of Novel Essential Genes in *Pseudomonas Aeruginosa*. *BMC Microbiol.* 14, 24.
- (11) Luo, H., Lin, Y., Gao, F., Zhang, C. T., and Zhang, R. (2014) DEG 10, an Update of the Database of Essential Genes That Includes Both Protein-Coding Genes and Noncoding Genomic Elements. *Nucleic Acids Res.* 42, D574.
- (12) Tremiño, L., Forcada-Nadal, A., and Rubio, V. (2018) Insight into Vitamin B6-Dependent Epilepsy Due to PLPBP (Previously PROSC) Missense Mutations. *Hum. Mutat.* 39, 1002–1013.
- (13) Eswaramoorthy, S., Gerchman, S., Graziano, V., Kycia, H., Studier, F. W., and Swaminathan, S. (2003) Structure of a Yeast Hypothetical Protein Selected by a Structural Genomics Approach. *Acta Crystallogr., Sect. D: Biol. Crystallogr.* 59, 127–135.
- (14) Tremiño, L., Forcada-Nadal, A., Contreras, A., and Rubio, V. (2017) Studies on Cyanobacterial Protein PipY Shed Light on Structure, Potential Functions, and Vitamin B6-Dependent Epilepsy. *FEBS Lett.* 591, 3431–3442.
- (15) Di Salvo, M. L., Safo, M. K., and Contestabile, R. (2012) Biomedical Aspects of Pyridoxal 5'-Phosphate Availability. *Front. Biosci., Elite Ed.* 4, 897–913.
- (16) Plecko, B., Zweier, M., Begemann, A., Mathis, D., Schmitt, B., Striano, P., Baethmann, M., Vari, M. S., Beccaria, F., Zara, F., Crowther, L. M., Joset, P., Sticht, H., Papuc, S. M., and Rauch, A. (2017) Confirmation of Mutations in PROSC as a Novel Cause of Vitamin B 6-Dependent Epilepsy. *J. Med. Genet.* 54, 809–814.
- (17) Shiraku, H., Nakashima, M., Takeshita, S., Khoo, C. S., Haniffa, M., Ch'ng, G. S., Takada, K., Nakajima, K., Ohta, M., Okanishi, T., Kanai, S., Fujimoto, A., Saitsu, H., Matsumoto, N., and Kato, M. (2018) PLPBP Mutations Cause Variable Phenotypes of Developmental and Epileptic Encephalopathy. *Epilepsia Open* 3, 495–502.
- (18) Roessler, S., Long, E. L., Budhu, A., Chen, Y., Zhao, X., Ji, J., Walker, R., Jia, H. L., Ye, Q. H., Qin, L. X., Tang, Z. Y., He, P., Hunter, K. W., Thorgerisson, S. S., Meltzer, P. S., and Wang, X. W. (2012) Integrative Genomic Identification of Genes on 8p Associated



with Hepatocellular Carcinoma Progression and Patient Survival. *Gastroenterology* 142, 957–966.

(19) Fux, A., Korotkov, V. S., Schneider, M., Antes, I., and Sieber, S. A. (2019) Chemical Cross-Linking Enables Drafting ClpXP Proximity Maps and Taking Snapshots of In Situ Interaction Networks. *Cell Chem. Biol.* 26, 48–59.

(20) Fux, A., Pfanzelt, M., Kirsch, V. C., Hoegl, A., and Sieber, S. A. (2019) Customizing Functionalized Cofactor Mimics to Study the Human Pyridoxal 5'-Phosphate-Binding Proteome. *Cell Chem. Biol.* 26, 1461–1468.

(21) Ahmed, S. A., McPhie, P., and Miles, E. W. (1996) A Thermally Induced Reversible Conformational Transition of the Tryptophan Synthase B2subunit Probed by the Spectroscopic Properties of Pyridoxal Phosphate and by Enzymatic Activity. *J. Biol. Chem.* 271, 8612–8617.

(22) Amorim Franco, T. M., Favrot, L., Vergnolle, O., and Blanchard, J. S. (2017) Mechanism-Based Inhibition of the Mycobacterium Tuberculosis Branched-Chain Aminotransferase by d - And l -Cycloserine. *ACS Chem. Biol.* 12, 1235–1244.

(23) Biasini, M., Bienert, S., Waterhouse, A., Arnold, K., Studer, G., Schmidt, T., Kiefer, F., Cassarino, T. G., Bertoni, M., Bordoli, L., and Schwede, T. (2014) SWISS-MODEL: Modelling Protein Tertiary and Quaternary Structure Using Evolutionary Information. *Nucleic Acids Res.* 42, 251–258.

(24) Dominguez, C., Boelens, R., and Bonvin, A. M. J. J. (2003) HADDOCK: A Protein-Protein Docking Approach Based on Biochemical or Biophysical Information. *J. Am. Chem. Soc.* 125, 1731–1737.

(25) Lowther, J., Yard, B. A., Johnson, K. A., Carter, L. G., Bhat, V. T., Raman, M. C. C., Clarke, D. J., Ramakers, B., McMahon, S. A., Naismith, J. H., and Campopiano, D. J. (2010) Inhibition of the PLP-Dependent Enzyme Serine Palmitoyltransferase by Cycloserine: Evidence for a Novel Decarboxylative Mechanism of Inactivation. *Mol. Biosyst.* 6, 1682–1693.

(26) Kao, A., Chiu, C., Vellucci, D., Yang, Y., Patel, V. R., Guan, S., Randall, A., Baldi, P., Rychnovsky, S. D., and Huang, L. (2011) Development of a Novel Cross-Linking Strategy for Fast and Accurate Identification of Cross-Linked Peptides of Protein Complexes. *Mol. Cell. Proteomics* 10, M110.002212.

(27) Liu, F., Rijkers, D. T. S., Post, H., and Heck, A. J. R. (2015) Proteome-Wide Profiling of Protein Assemblies by Cross-Linking Mass Spectrometry. *Nat. Methods* 12, 1179–1184.

(28) Arnold, K., Bordoli, L., Kopp, J., and Schwede, T. (2006) The SWISS-MODEL Workspace: A Web-Based Environment for Protein Structure Homology Modelling. *Bioinformatics* 22, 195–201.

(29) Wang, X., Cimermanic, P., Yu, C., Schweitzer, A., Chopra, N., Engel, J. L., Greenberg, C., Huszagh, A. S., Beck, F., Sakata, E., Yang, Y., Novitsky, E. J., Leitner, A., Nanni, P., Kahraman, A., Guo, X., Dixon, J. E., Rychnovsky, S. D., Aebersold, R., Baumeister, W., Salii, A., and Huang, L. (2017) Molecular Details Underlying Dynamic Structures and Regulation of the Human 26S Proteasome. *Mol. Cell. Proteomics* 16, 840–854.

(30) Ashburner, M., Ball, C. A., Blake, J. A., Botstein, D., Butler, H., Cherry, J. M., Davis, A. P., Dolinski, K., Dwight, S. S., Eppig, J. T., Harris, M. A., Hill, D. P., Issel-Tarver, L., Kasarskis, A., Lewis, S., Matese, J. C., Richardson, J. E., Ringwald, M., Rubin, G. M., and Sherlock, G. (2000) Gene Ontology: Tool for the Unification of Biology. *Nat. Genet.* 25, 25–29.

(31) Tovey, C. A., and Conduit, P. T. (2018) Microtubule Nucleation by  $\gamma$ -Tubulin Complexes and Beyond. *Essays Biochem.* 62, 765–780.

(32) Brunk, K., Zhu, M., Bärenz, F., Kratz, A. S., Haselmann-Weiss, U., Antony, C., and Hoffmann, I. (2016) Cep78 Is a New Centriolar Protein Involved in Plk4-Induced Centriole Overduplication. *J. Cell Sci.* 129, 2713–2718.

(33) Spektor, A., Tsang, W. Y., Khoo, D., and Dynlacht, B. D. (2007) Cep97 and CP110 Suppress a Cilia Assembly Program. *Cell* 130, 678–690.

(34) Le Clech, M. (2008) Role of CAP350 in Centriolar Tubule Stability and Centriole Assembly. *PLoS One* 3, e3855.

(35) Yan, X., Habedanck, R., and Nigg, E. A. (2006) A Complex of Two Centrosomal Proteins, CAP350 and FOP, Cooperates with EB1 in Microtubule Anchoring. *Mol. Biol. Cell* 17, 634–644.

(36) Kleylein-Sohn, J., Westendorf, J., Le Clech, M., Habedanck, R., Stierhof, Y. D., and Nigg, E. A. (2007) Plk4-Induced Centriole Biogenesis in Human Cells. *Dev. Cell* 13, 190–202.

(37) Chen, Z., Indjeian, V. B., McManus, M., Wang, L., and Dynlacht, B. D. (2002) CP110, a Cell Cycle-Dependent CDK Substrate, Regulates Centrosome Duplication in Human Cells. *Dev. Cell* 3, 339–350.

(38) Li, J., D'Angiolella, V., Seeley, E. S., Kim, S., Kobayashi, T., Fu, W., Campos, E. I., Pagano, M., and Dynlacht, B. D. (2013) USP33 Regulates Centrosome Biogenesis via Deubiquitination of the Centriolar Protein CP110. *Nature* 495, 255–259.

(39) Narita, A., Takeda, S., Yamashita, A., and Maéda, Y. (2006) Structural Basis of Actin Filament Capping at the Barbed-End: A Cryo-Electron Microscopy Study. *EMBO J.* 25, 5626–5633.

(40) Hayes, M. J., Rescher, U., Gerke, V., and Moss, S. E. (2004) Annexin-Actin Interactions. *Traffic* 5, 571–576.

(41) Janji, B., Giganti, A., De Corte, V., Catillon, M., Bruyneel, E., Lentz, D., Plastino, J., Gettemans, J., and Friederich, E. (2006) Phosphorylation on Ser5 Increases the F-Actin-Binding Activity of L-Plastin and Promotes Its Targeting to Sites of Actin Assembly in Cells. *J. Cell Sci.* 119, 1947–1960.

(42) Rayment, I., Holden, H. M., Whittaker, M., Yohn, C. B., Lorenz, M., Holmes, K. C., and Milligan, R. A. (1993) Structure of the Actin-Myosin Complex and Its Implications for Muscle Contraction. *Science* 261, 58–65.

(43) Goellner, B., and Aberle, H. (2012) The Synaptic Cytoskeleton in Development and Disease. *Dev. Neurobiol.* 72, 111–125.

(44) Kamijo, K., Ohara, N., Abe, M., Uchimura, T., Hosoya, H., Lee, J. S., and Miki, T. (2006) Dissecting the Role of Rho-Mediated Signaling in Contractile Ring Formation. *Mol. Biol. Cell* 17, 43–55.

(45) Zhang, X., and Bian, J. S. (2014) Hydrogen Sulfide: A Neuromodulator and Neuroprotectant in the Central Nervous System. *ACS Chem. Neurosci.* 5, 876–883.

(46) Veeranki, S., and Tyagi, S. C. (2015) Role of Hydrogen Sulfide in Skeletal Muscle Biology and Metabolism. *Nitric Oxide* 46, 66–71.

(47) Haren, L., Remy, M. H., Bazin, I., Callebaut, I., Wright, M., and Merdes, A. (2006) NEDD1-Dependent Recruitment of the  $\gamma$ -Tubulin Ring Complex to the Centrosome Is Necessary for Centriole Duplication and Spindle Assembly. *J. Cell Biol.* 172, 505–515.

(48) Ito, T., Yamamoto, K., Hori, R., Yamauchi, A., Downs, D. M., Hemmi, H., and Yoshimura, T. (2019) Conserved Pyridoxal 5'-Phosphate-Binding Protein YggS Impacts Amino Acid Metabolism through Pyridoxine 5'-Phosphate in Escherichia Coli. *Appl. Environ. Microbiol.* 85 (11), e00430-19.

(49) Kulak, N. A., Pichler, G., Paron, I., Nagaraj, N., and Mann, M. (2014) Minimal, Encapsulated Proteomic-Sample Processing Applied to Copy-Number Estimation in Eukaryotic Cells. *Nat. Methods* 11, 19–24.

(50) Phillips, R. S. (2015) Chemistry and Diversity of Pyridoxal-5'-Phosphate Dependent Enzymes. *Biochim. Biophys. Acta, Proteins Proteomics* 1854, 1167–1174.

(51) Linster, C. L., Van Schaftingen, E., and Hanson, A. D. (2013) Metabolite Damage and Its Repair or Pre-Emption. *Nat. Chem. Biol.* 9, 72–80.

(52) Vizcaino, J. A., Csordas, A., Del-Toro, N., Dianes, J. A., Griss, J., Lavidas, I., Mayer, G., Perez-Riverol, Y., Reisinger, F., Terment, T., Xu, Q. W., Wang, R., and Hermjakob, H. (2016) 2016 Update of the PRIDE Database and Its Related Tools. *Nucleic Acids Res.* 44, 447–456.